Real-Time Control of a 2-DoF Helicopter Via Model Matching H_∞ Matrix Modulation Approach

(H_∞ Control of a Laboratory Helicopter: A Matrix Modulation Approach)

Parthish Kumar Paul
Research Scholar, Dept. of Electrical Engineering
National Institute of Technology Calicut
Calicut – 673601, India
E-mail: parthish.k@gmail.com

Jeevamma Jacob
Professor, Dept. of Electrical Engineering
National Institute of Technology Calicut
Calicut – 673601, India
E-mail: jeeva@nitc.ac.in

***Abstract*—This paper addresses the convergence issues of the H_∞ control algorithm by a matrix modulation technique on the mathematical generalized plant model of a system. This paper further presents a general solution to the robust control algorithm convergence problem of MIMO systems. The proposed controller is optimized for output error regulation by comparing the outputs of a higher order MIMO system to that of a slightly underdamped second order plant. The matrix modulation approach considers two singularities, viz., 1) control singularity; and 2) sensor singularity. The corresponding controller is tested on a laboratory model of helicopter, known as Twin Rotor MIMO System (TRMS) for its take off and hovering.**

Keywords—Matrix modulation; Twin Rotor MIMO System (TRMS); singularity; generalized plant; H_∞ control; output error regulation

I. INTRODUCTION

In the recent decades, a trend of replacing mechanical (hydraulic and pneumatic) elements by more sophisticated electrical elements is being observed in rotorcraft technology. This change is necessitated because of the need to produce light weight maintenance free vehicles for unmanned autonomous flights. This move has lead to distinguished changes in flight dynamics of such vehicles leading to increase in its electrical complexity while reducing overall size and weight of the system. Thus, this transition is motivated by the effectiveness in weight, volume, fuel and maintenance. Due to light weight of these vehicles, new prototypes are replacing the traditional fossil fuel driven rotorcraft for catering specific tasks. Neo-models are driven by battery sources. Again, due to these alterations, control challenges have now acquired higher dimensions. Such modifications have lead to the revelation of new system dynamics projecting the need to address the control problems for this class of systems differently. Such systems find its importance from control perspective as they exhibit specific attributes that pose serious control challenges. These challenges are due to non-minimum phase dynamics, cross coupling, model uncertainties, sensitivity to exogenous disturbances, sensor singularities, control singularities, and resonances. The available robust control tools of mathematical solvers very well take care of the aforementioned attributes except the singularity issues in specific cases. Due to singularities in certain signals resulting in matrix singularities at particular frequencies, the robust control algorithms fail to converge in typical cases. The robust H_∞ control design is based on the structure of a generalized plant (mathematical design) that subsumes all subsystems (except the controller) including the actual plant (the linear model). The present work proposes a modulation in the mathematical framework of the generalized plant, specially certain matrix representations, ensuring convergence of the algorithm.

The Twin Rotor Multi Input Multi Output System (TRMS), developed by Feedback Instruments Ltd., is an ideal test bench in this experiment as it exhibits all such attributes as cited above. It is a laboratory model of helicopter with 2 Degrees of Freedom (DoF). Fig. 1 illustrates TRMS in the laboratory without excitation. Fig. 2 is the working model of TRMS in hovering mode. TRMS travels in two planes mutually perpendicular to each other. The two rotors of TRMS are in these planes and rotate with a comparatively faster dynamics as compared to the rigid body movements. So, rotor dynamics are decoupled from rigid body dynamics by design.

The moment due to main rotor has strong impact on the yaw (angular displacement of tail around pivot axis) angle, while that due to tail rotor has weak effect on the pitch (elevation) angle of TRMS. This incorporates strong cross coupled dynamics. In addition, TRMS has RHP (Right Half Plane) zero dynamics and resonant modes, as in [1]-[4]. Due to model intricacy, the system acquires higher order. At the same time, critical dynamics are inadvertently ignored during linear modeling in most of the cases, as in [4]. Thus, model uncertainty is inevitable. Like other flying vehicles, atmospheric turbulence needs to be considered here as output disturbance. Hence, TRMS falls in the class of systems as considered in this paper. The control singularity at infinite (very high) frequency and sensor singularity at zero (infinitesimally small) frequency lead to yielding certain non-invertible matrices at some intermediate stages while computer iteration of the control algorithms is executed. This issue is addressed in the present work.

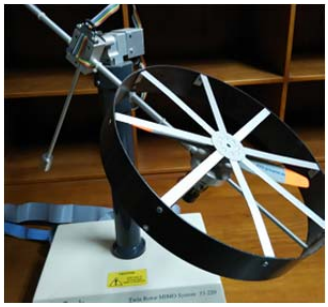

Fig. 1. TRMS in the laboratory without excitation.

Fig. 2. TRMS in the laboratory while hovering.

The solution to the H_∞ control problem had been explored to its entirety during the last decades of 20th century. The control theory of H_∞ optimization developed steeply but gradually during that period. Salient properties of sensitivity reducing scheme were presented by Zames [5]. Complete characterization of four block plant structure by algebraic Riccati equations was worked out by Zhou and Khargonekar [6]. Contemporary to this, a detailed derivation of output feedback H_∞ controller was presented, as in [7]. Iwasaki and Skelton solved a general H_∞ control problem by parameterization in state space using linear matrix inequality, as in [8]. Doyle presented Riccati equation based solution to the H_∞ control problem, as in [9]. The modern day H_∞ controller iteration tools refer to this work [9] for norm based optimization. In another work, it was established that finite order controller may be obtained only with redundant value of constraint [10], that is, the norm. In all contemporary works of that period, H_∞ optimization algorithms were developed mathematically, starting from the basics. But, the limitation of the generalized plant in solving the systems with singularity issues was sparsely addressed. These issues are tackled in this paper by modulating the generalized plant matrix representation via suitable augmentation with certain signals. The control algorithms thus converge and stabilizing H_∞ controllers are obtained and tested on TRMS in real time.

Classical linear control of TRMS or this class of systems by pole zero cancellation is not suitable due to RHP zero dynamics and cross coupling issues, as in [11]-[13]. Toha and Tohki attempted to determine an inverse model based PID controller with limited performance indicators, as in [14]. In another attempt, hybrid robust control in conjunction with sliding mode control was tested on TRMS with less clear simulation results of real time tracking and control, as in [15]. In an erstwhile work by the authors of the present work, simulation results of robust control were presented using a simple state space model of TRMS emphasizing the need of gravity compensation, as in [16]. No details of generalized plant restructuring and real time application were provided in that work. Further, the physical plants characterizing this class of systems are nonlinear in nature, as in [17]. In another attempt, optimal control of decoupled SISO TRMS is presented, as in [18]. These facts, jointly with modeling uncertainties, make TRMS like systems hard to control by standard techniques. Due to model uncertainties and missing critical dynamics, there is marked difference between the actual plant and the corresponding Linear Time Invariant (LTI) models. Thus, H_∞ robust control techniques are deemed fit to address the control problem in the present work. In this work, the LTI model is obtained from the nonlinear mathematical model of the system. Subsequently, the robust controllers are designed based on the derived nominal model.

The present paper considers vector augmentation of the four block plant structure for certain mathematical correction to address the matrix singularity issues in the inclusive mathematical plant called as the generalized plant. Refer to a former work, as in [6]. Details of the matrix modulation technique in conjunction with the existing four block plant structure and robust control technique leading to a converging controller design approach are presented in this work. The mathematical modulation made to the four block generalized plant is validated by designing a robust H_∞ controller and flying the TRMS in the closed loop mode.

The control objective is to achieve the relative and absolute stability parameters and minimize the effects of disturbances at the plant outputs in the real time. In order to achieve these objectives a model matching problem is considered, where the relative and absolute stability specifications are stipulated using a second order reference plant. Simulation and real time experimental results of the closed loop TRMS illustrate reference tracking and robust stability during take off and hovering.

LTI modeling of TRMS is presented in Section II. Details of generalized plant restructuring by mathematical modulation are presented in Section III. The restructured generalized plant is used in designing the H_∞ controllers as revealed in Section IV. The simulation results are presented and discussed in Section V. Conclusion is given in Section VI.

II. LINEARIZATION OF TRMS

The mathematical model of TRMS, as presented in [19], is restated below for ease of reference.

A. Moments in the vertical plane

The moments and angular displacements of TRMS are illustrated in vector form in Fig. 3. The nonlinear equations in time domain pertaining to the pitch movement of TRMS are quoted from (1) through (6) below:

$$I_1.\ddot{\psi} = M_1 - M_{FG} - M_{B\psi} - M_G \quad (1)$$

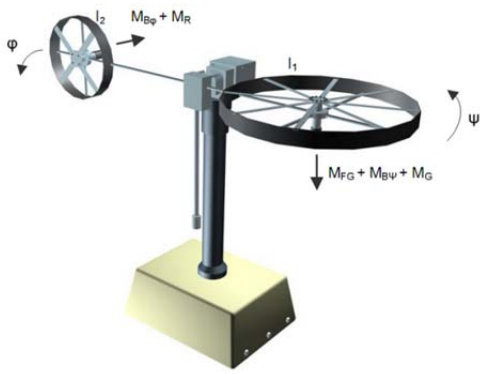

Fig. 3. Illustration of angular displacements and moments of TRMS while hovering [19].

TABLE I. NOMENCLATURE

Sl. No.	Nomenclature and Definitions	
	Terms	***Definition***
1.	Ψ	pitch (elevation) angle
2.	M_1	nonlinear static momentum in horizontal plane
3.	M_{FG}	gravity momentum
4.	$M_{B\Psi}$	friction forces momentum in horizontal plane
5.	M_G	gyroscopic momentum in horizontal plane
6.	τ_M	main motor torque
7.	u_M	main motor control input
8.	φ	yaw (tail displacement) angle
9.	M_2	nonlinear static momentum in vertical plane
10.	$M_{B\varphi}$	friction forces momentum in vertical plane
11.	M_R	cross reaction momentum in vertical plane
12.	τ_T	tail motor torque
13.	u_T	tail motor control input

TABLE II. COEFFICIENTS

Sl. No.	Coefficients and Values	
	Coefficient	***Values***
1.	I_1 – moment of inertia of vertical rotor	6.8×10-2 kg.m2
2.	I_2 – moment of inertia of horizontal rotor	2×10-2 kg.m2
3.	a_1 – static characteristic parameter	0.0135
4.	b_1 - static characteristic parameter	0.0924
5.	a_2 – static characteristic parameter	0.02
6.	b_2 - static characteristic parameter	0.09
7.	Mg – gravity momentum	0.32 N-m
8.	$B_{1\psi}$ – friction momentum function parameter	6×10-3 N-m-s/rad.
9.	$B_{2\psi}$ – friction momentum function parameter	1×10-3 N-m-s/rad.
10.	$B_{1\varphi}$ – friction momentum function parameter	1×10-1 N-m-s/rad.
11.	$B_{2\varphi}$ – friction momentum function parameter	1×10-2 N-m-s/rad.
12.	Kgy – gyroscopic momentum parameter	0.05 sec/rad.
13.	k_1 – motor 1 gain	1.1
14.	K_2 – motor 2 gain	0.8
15.	T_{11} – motor 1 denominator parameter	1.1
16.	T_{10} – motor 1 denominator parameter	1
17.	T_{21} – motor 2 denominator parameter	1
18.	T_{20} – motor 2 denominator parameter	1
19.	Tp – cross reaction momentum parameter	2
20.	T_0 – cross reaction momentum parameter	3.5
21.	Kc – cross reaction momentum gain	-0.2

$$M_1 = a_1.{\tau_M}^2 + b_1.\tau_M \quad (2)$$

Important variables and terms used in (1) through (11) are defined in Table 1. Values assigned to different coefficients used in (1) through (11) are shown in Table 2. Main rotor of TRMS provides necessary thrust for pitch. Rest position of pitch rotor in vertical plane is balanced by a counter weight, which is modeled by choice, to set the angle of elevation as desired. The weight and position of counter weight provide necessary inputs for designing the gravity compensation block, to be used in feed forward compensation during flight [16].

$$M_{FG} = M_g.\sin(\psi) \quad (3)$$

$$M_{B\psi} = B_{1\psi}.\dot{\psi} + B_{2\psi}.sign(\dot{\psi}) \quad (4)$$

$$M_G = K_{gy}.M_1.\dot{\varphi}.\cos(\psi) \quad (5)$$

$$T_{11}\dot{\tau}_M = -T_{10}\tau_M + k_1 u_M \quad (6)$$

B. Moments in the horizontal plane

The nonlinear equations in time domain pertaining to the yaw movement of TRMS are quoted from (7) through (11).

$$I_2.\ddot{\varphi} = M_2 - M_{B\varphi} - M_R \quad (7)$$

$$M_2 = a_2.{\tau_T}^2 + b_2.\tau_T \quad (8)$$

$$M_{B\varphi} = B_{1\varphi}.\dot{\psi} + B_{2\varphi}.sign(\dot{\varphi}) \quad (9)$$

$$T_p\dot{M}_R = k_c T_0 \dot{\tau}_M + k_c\tau_M - M_R \quad (10)$$

$$T_{21}\dot{\tau}_T = -T_{20}\tau_T + k_2 u_T \quad (11)$$

Equations (1) through (11) completely determine the nonlinear behavior of TRMS. The coefficients in Table 2 are determined from the design time estimates of TRMS.

A nominal model of TRMS is obtained by linearizing the nonlinear dynamic mathematical model of TRMS presented in (1) through (11). The nonlinear model of TRMS is linearized around an equilibrium point (the origin) by finding its Jacobians. Partial time derivative terms in the mathematical expressions are considered for first order differentiation. Second and higher order terms are neglected in state space modeling due to nominal values. One distinct advantage of robust control approach is that the controller design is least

affected by the marked difference between the nominal model and the actual plant. Thus, the missing dynamics of the system are taken care of by the controller algorithm. The given system (TRMS) yields seven state variables. The state vector is defined as '*X*'. In this paper, all variables are in SI units except the presentation of angular displacements (illustrated pictorially in degrees for ease of interpretation).

The state space model may be obtained as:

$$\dot{X} = AX + BU \tag{12}$$

$$Y = CX + DU \tag{13}$$

Where,

$$X = [\psi \quad \varphi \quad \dot{\psi} \quad \dot{\varphi} \quad \tau_M \quad \tau_T \quad M_R]^T \tag{14}$$

i.e., $$X = [x_1 \quad x_2 \quad x_3 \quad x_4 \quad x_5 \quad x_6 \quad x_7]^T \tag{15}$$

where $\dot{\psi}$ is rate of change of pitch angle, and $\dot{\varphi}$ is rate of change of yaw angle. (Other variables are defined in Table 1.) The variables $x_1 - x_7$ are the corresponding state variables.

The input vector is given as $U = [u_M \quad u_T]^T$ (16)

The output vector is defined as $Y = [\psi \quad \varphi]^T$ (17)

The matrices A, B, C and D in (12) and (13) may be given as,

$$A = \begin{bmatrix} A_{11} & A_{12} \\ A_{21} & A_{22} \end{bmatrix}, B = \begin{bmatrix} 0 & 0 & 0 & 0 & \frac{k_1}{T_{11}} & 0 & \frac{T_0 k_c k_1}{T_p T_{11}} \\ 0 & 0 & 0 & 0 & 0 & \frac{k_2}{T_{21}} & 0 \end{bmatrix}^T$$

$$C = \begin{bmatrix} 1 & 0 & 0 & 0 & 0 & 0 & 0 \\ 0 & 1 & 0 & 0 & 0 & 0 & 0 \end{bmatrix}, D = \begin{bmatrix} 0 & 0 \\ 0 & 0 \end{bmatrix}$$

$$A_{11} = \begin{bmatrix} 0 & 0 & 1 & 0 \\ 0 & 0 & 0 & 1 \\ -M_G/I_1 & 0 & (-B_{1\psi}/I_1 - 2B_{2\psi}/I_1) & 0 \\ 0 & 0 & -B_{1\varphi}/I_2 & -B_{2\varphi}/I_2 \end{bmatrix}$$

$$A_{12} = \begin{bmatrix} 0 & 0 & 0 \\ 0 & 0 & 0 \\ b_1/I_1 & 0 & 0 \\ 0 & b_2/I_2 & -1/I_2 \end{bmatrix}, A_{21} = \begin{bmatrix} 0 & \dots & 0 \\ \vdots & \ddots & \vdots \\ 0 & \dots & 0 \end{bmatrix}_{3\times 4}$$

$$A_{22} = \begin{bmatrix} -T_{10}/T_{11} & 0 & 0 \\ 0 & -T_{21}/T_{21} & 0 \\ (k_c/T_p) \times (1 - T_0 T_{10}/T_{11}) & 0 & -1/T_p \end{bmatrix} \tag{18}$$

The state space representation of the plant is made use of in defining the generalized plant. A general form of the generalized plant is presented in the following section.

III. Generalized Plant Resrtucturing by Matrix Modulation

Interconnection of the generalized plant, P(s) (to be formulated) with controller, K(s) and Inputs/Outputs (I/O's) is illustrated in Fig. 4. With the availability of state space model of a given system like TRMS, structuring of the generalized plant (four block) is the next step in H_∞ robust controller design. The input vectors W(s) and U(s) stand for the exogenous/disturbance inputs and control inputs, respectively. The output vectors Z(s) and Y(s) are the regulated error signals and generalized plant outputs, respectively. By definition, I/O's of the generalized plant may differ from those of the physical plant. Refer to Skogestad and Postlethwaite in [20] for a detailed account on the generalized plant formulation.

Consider a plant with m_1 exogenous inputs, $w_1, w_2, w_3, \dots, w_{m_1}$ and m_2 control inputs, $u_1, u_2, u_3, \dots, u_{m_2}$. Similarly, consider this plant with p_1 regulated outputs, $z_1, z_2, z_3, \dots, z_{p_1}$ and p_2 measured outputs, $y_1, y_2, y_3, \dots, y_{p_2}$.

That is

$$W(t) = [w_1 \quad w_2 \quad w_3 \quad \cdots \quad w_{m_1}]^T \tag{19}$$

$$U(t) = [u_1 \quad u_2 \quad u_3 \quad \cdots \quad u_{m_2}]^T \tag{20}$$

$$Z(t) = [z_1 \quad z_2 \quad z_3 \quad \cdots \quad z_{p_1}]^T \tag{21}$$

$$Y(t) = [y_1 \quad y_2 \quad y_3 \quad \cdots \quad y_{p_2}]^T \tag{22}$$

The p×m generalized plant system may be presented in state space as

$$\dot{X}(s) = AX(s) + B_1 W(s) + B_2 U(s) \tag{23}$$

$$Z(s) = C_1 X(s) + D_{11} W(s) + D_{12} U(s) \tag{24}$$

$$Y(s) = C_2 X(s) + D_{21} W(s) + D_{22} U(s) \tag{25}$$

The generalized plant, P(t) in packed form may be given as

$$P(t) = \begin{bmatrix} [A] & [B_1 \quad B_2] \\ \begin{bmatrix} C_1 \\ C_2 \end{bmatrix} & \begin{bmatrix} D_{11} & D_{12} \\ D_{21} & D_{22} \end{bmatrix} \end{bmatrix} \tag{26}$$

$$\xrightarrow{yields} P(s) = \begin{bmatrix} C_1 \\ C_2 \end{bmatrix} [sI - A]^{-1} [B_1 \quad B_2] + \begin{bmatrix} D_{11} & D_{12} \\ D_{21} & D_{22} \end{bmatrix} \tag{27}$$

Singularity of the sub-matrices is an unavoidable cause of premature termination of control algorithms. As we consider sensor singularity at zero frequency and control singularity at infinite frequency, the matrices D_{21} and D_{12} need special attention. In case, D_{12} has dependent columns, full columns rank (m_2) cannot be retained. This fact leads to control singularities as one or more control signal(s) is/are prohibited from affecting the state. Similarly, when D_{21} has dependent rows, full row rank (p_2) may fall short. Thus, sensor singularities occur because one or more output(s) is/are not measurable during estimation. In the present work, such singularities are taken care of by considering mathematical augmentations in the generalized plant leading to correction in the conventional structure. The H_∞ controller optimization algorithm is not affected by this correction.

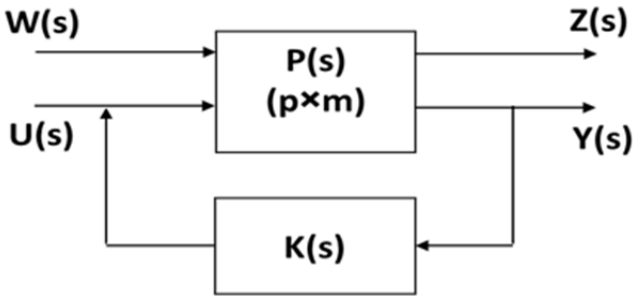

Fig. 4. Control configuration of the generalized plant.

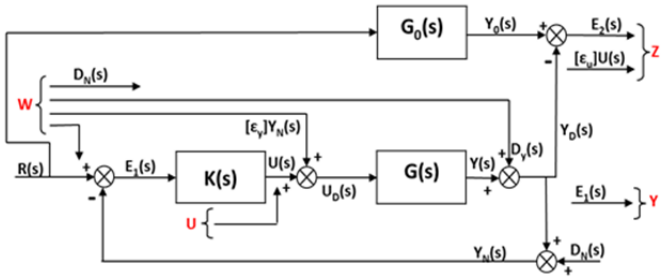

Fig. 5. Singularity treated general structure.

A second order reference plant, $G_0(s)$ with slightly underdamped responses is considered to specify the desired responses. Thus, output error regulation approach is used to optimize the control algorithms. A singularity treated general structure of the generalized plant along with the controller is presented in Fig. 5. The four exogenous input vectors are illustrated, viz. measurement noise, output disturbance, weighted measurement noise, and reference input. The other input is the control vector, $U(s)$. The output error between the reference plant and the actual plant is considered as vector $Z(s)$, to be regulated. The difference between the measured output and the reference input is considered as the generalized plant output, $E_1(s)$. Control singularity is mitigated by augmenting the weighted control signal, $[\varepsilon_u]U(s)$ to the output signal, $Z(s)$ by regulation. $[\varepsilon_u]$ is a $m_2 \times m_2$ diagonal matrix. Similarly, sensor singularity is mitigated by augmenting the weighted measured output, $[\varepsilon_y]Y_N(s)$ to the control signal $U(s)$. $[\varepsilon_y]$ is a $m_2 \times p_2$ diagonal non-square matrix. Orders of the matrices and vectors are shown in Table 3. Thus, we have

$$W(s) = [W]_{(m_1+m_2)\times 1},\ U(s) = [U]_{m_2\times 1},$$

$$Z(s) = [Z]_{(p_1+m_2)\times 1},\ Y(s) = [Y]_{p_2\times 1}.$$

From (27), the generalized plant may be obtained as a four block plant as shown below:

$$P(s) = \begin{bmatrix} P_A & P_B \\ P_C & P_D \end{bmatrix}, \text{where } P_A = \begin{bmatrix} P_{A11} & P_{A12} \\ P_{A21} & P_{A22} \end{bmatrix},$$

$$P_B = [P_{B1} \quad P_{B2}]^T, \text{and } P_C = [P_{C1} \quad P_{C2}] \tag{28}$$

Further, defining each sub-matrices,

TABLE III. ORDERS – VECTORS AND MATRICES

Sl. No.	Vector and Matrix Order	
	Vector/Matrix Name	*Order*
1.	No. of states of $G(s)$	n
2.	No. of states of $G_0(s)$	n_0
3.	No. of exogenous inputs	m_1
4.	No. of control inputs	m_2
5.	No. of regulated outputs	p_1
6.	No. of measured outputs	p_2
7.	Order of A	$(n + n_0)\times(n + n_0)$
8.	Order of B_1	$(n + n_0)\times(m_1 + m_2)$
9.	Order of B_2	$(n + n_0)\times(m_2)$
10.	Order of C_1	$(p_1 + m_2)\times(n + n_0)$
11.	Order of C_2	$p_2\times(n + n_0)$
12.	Order of D_{11}	$(p_1 + m_2)\times(m_1 + m_2)$
13.	Order of D_{12}	$(p_1 + m_2)\times m_2$
14.	Order of D_{21}	$p_2\times(m_1 + m_2)$
15.	Order of D_{22}	$p_2\times m_2$

*$p_1 = p_2 + m_2$; $m_1 = p_2 + m_2$

$$P_{A11} = \begin{bmatrix} G_{01} & 0 & \cdots & 0 & 0 \\ 0 & G_{02} & 0 & \cdots & 0 \\ \cdots & 0 & \cdots & 0 & \cdots \\ 0 & \cdots & 0 & \cdots & 0 \\ 0 & 0 & \cdots & 0 & G_{0p2} \end{bmatrix}_{(p_2\times p_2)}$$

$$P_{A12} = \begin{bmatrix} -G_{11}\varepsilon_{Y1} & -G_{12}\varepsilon_{Y2} & \cdots & \cdots & -G_{1m_2}\varepsilon_{Ym_2} \\ -G_{21}\varepsilon_{Y1} & -G_{21}\varepsilon_{Y2} & \cdots & \cdots & -G_{2m_2}\varepsilon_{Ym_2} \\ \cdots & \cdots & \cdots & \cdots & \cdots \\ \cdots & \cdots & \cdots & \cdots & \cdots \\ -G_{p_21}\varepsilon_{Y1} & -G_{p_21}\varepsilon_{Y2} & \cdots & \cdots & -G_{p_2m_2}\varepsilon_{Ym_2} \end{bmatrix}_{(p_2\times m_2)}$$

$$P_{A21} = [0]_{m_2\times p_2},\ P_{A22} = [0]_{m_2\times m_2}$$

$$P_{B1} = \begin{bmatrix} -G_{11} & -G_{12} & \cdots & \cdots & -G_{1m_2} \\ -G_{21} & -G_{22} & \cdots & \cdots & -G_{2m_2} \\ \cdots & \cdots & \cdots & \cdots & \cdots \\ \cdots & \cdots & \cdots & \cdots & \cdots \\ -G_{p_21} & -G_{p_22} & \cdots & \cdots & -G_{p_2m_2} \end{bmatrix}_{(p_2\times m_2)}$$

$$\varepsilon_U = \begin{bmatrix} \varepsilon_{U_1} & 0 & \cdots & 0 & 0 \\ 0 & \varepsilon_{U_2} & 0 & \cdots & 0 \\ \cdots & 0 & \cdots & 0 & \cdots \\ 0 & \cdots & 0 & \cdots & 0 \\ 0 & 0 & \cdots & 0 & \varepsilon_{U_{m_2}} \end{bmatrix}_{(m_2\times m_2)},\ P_{B2} = \varepsilon_U \tag{29}$$

$$P_{C1} = [Identity\ Matrix]_{p_2\times p_2},\ P_{C2} = P_{A12},\ P_D = P_{B1}$$

$$\varepsilon_Y = \begin{bmatrix} \varepsilon_{Y1} & 0 & \cdots & \cdots & \cdots & \cdots & 0 & 0 \\ 0 & \varepsilon_{Y2} & 0 & \cdots & \cdots & \cdots & \cdots & 0 \\ \cdots & 0 & \cdots & 0 & \cdots & \cdots & \cdots & \cdots \\ 0 & \cdots & 0 & \cdots & 0 & \cdots & \cdots & 0 \\ 0 & 0 & \cdots & 0 & \varepsilon_{Y_{m_2}} & 0 & 0 & 0 \end{bmatrix}_{m_2 \times p_2} \quad \forall m_2 \leq p_2 \tag{30}$$

$$G_0(s) = P_{A11}, G_{0k}(s) = G_{ak}\,({\omega_{nk}}^2)/(s^2 + 2\xi_k\omega_{nk}s + {\omega_{nk}}^2)$$

Where, $k = 1,2,3,\ldots p_2$. (31)

The plant transfer function, $G_{Plant}(s) = -P_{B1}$ (32)

IV. Designing of H_∞ Controller

The objective of H_∞ optimization algorithm is to minimize the respective norms of the closed loop transfer matrix $T_{ZW}(s)$ from $W(s)$ to $Z(s)$ for a given generalized plant $P(s)$, as in [10]. The H_∞ optimization algorithm yields a strictly proper controller for a suboptimal norm (γ>1) on $T_{ZW}(s)$. Thus, the H_∞ optimization problem may be stated as finding a stabilizing controller, K(s) with constraint on loop transfer function, $T_{ZW}(s)$, as in [21]. Mathematically,

$\|T_{ZW}(s)\|_\infty < \gamma, \gamma \geq 1\forall$ strictly proper H_∞ controller.

The mathematically modulated generalized plant structure presented in Section III may be simplified in order to design a controller for TRMS. Fig. 5 is redrawn with TRMS as the actual plant and illustrated in Fig. 6. Orders of the vectors and matrices are shown in Table 4. Thus, we have

$$W(s) = [W]_{4\times1}, U(s) = [U]_{2\times1},$$
$$Z(s) = [Z]_{4\times1}, Y(s) = [Y]_{2\times1}.$$
$$\varepsilon_Y = \begin{bmatrix} \varepsilon_{Y_1} & 0 \\ 0 & \varepsilon_{Y_2} \end{bmatrix}_{2\times2}, \varepsilon_U = \begin{bmatrix} \varepsilon_{U_1} & 0 \\ 0 & \varepsilon_{U_2} \end{bmatrix}_{2\times2}.$$

Thus, the generalized plant is obtained as

$$P(s) = \begin{bmatrix} \begin{bmatrix} G_{01} & 0 & -G_{11}\varepsilon_{Y_1} & -G_{12}\varepsilon_{Y_2} \\ 0 & G_{02} & -G_{21}\varepsilon_{Y_1} & -G_{22}\varepsilon_{Y_2} \\ 0 & 0 & 0 & 0 \\ 0 & 0 & 0 & 0 \end{bmatrix} & \begin{bmatrix} -G_{11} & -G_{12} \\ -G_{21} & -G_{22} \\ \varepsilon_{U_1} & 0 \\ 0 & \varepsilon_{U_2} \end{bmatrix} \\ \begin{bmatrix} 1 & 0 & -G_{11}\varepsilon_{Y_1} & -G_{12}\varepsilon_{Y_2} \\ 0 & 1 & -G_{21}\varepsilon_{Y_1} & -G_{22}\varepsilon_{Y_2} \end{bmatrix} & \begin{bmatrix} -G_{11} & -G_{12} \\ -G_{21} & -G_{22} \end{bmatrix} \end{bmatrix}$$

$$G_{01}(s) = G_{a1}\,({\omega_{n1}}^2)/(s^2 + 2\xi_1\omega_{n1}s + {\omega_{n1}}^2)$$
$$G_{02}(s) = G_{a2}\,({\omega_{n2}}^2)/(s^2 + 2\xi_2\omega_{n2}s + {\omega_{n2}}^2)$$

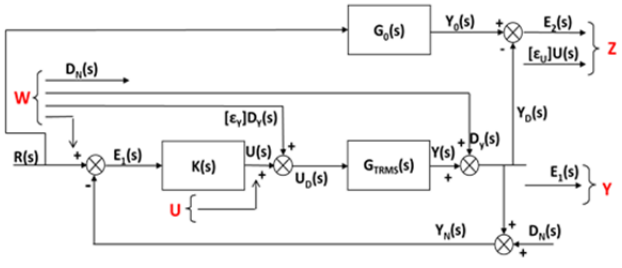

Fig. 6. Singularity treated TRMS.

TABLE IV. Orders – Vectors and Matrices

Sl. No.	Vector and Matrix Order	
	Vector/Matrix Name	*Order*
1.	No. of states of $G(s)$	7
2.	No. of states of $G_0(s)$	4
3.	No. of exogenous inputs	2*
4.	No. of control inputs	2
5.	No. of regulated outputs	4
6.	No. of measured outputs	2
7.	Order of A	11×11
8.	Order of B_1	11×4
9.	Order of B_2	11×2
10.	Order of C_1	4×11
11.	Order of C_2	2×11
12.	Order of D_{11}	4×4
13.	Order of D_{12}	4×2
14.	Order of D_{21}	2×4
15.	Order of D_{22}	2×2

*Output disturbance and measurement noise vectors are ignored in this design for simplicity.

For computer programming, values are assigned from Table 2 into (18). The generalized plant is defined in time domain from (26) and used as it is for defining programming parameters. Other values are mentioned below:

$$\varepsilon_{U_1} = \varepsilon_{U_2} = 0.01, \varepsilon_{Y_1} = \varepsilon_{Y_2} = 0.01, \xi_1 = \xi_2 = 0.9$$
$$\omega_{n_1} = \omega_{n_2} = 0.5, G_{a_1} = 1.02, G_{a_2} = 0.01$$

A suboptimal H_∞ controller is obtained by computer iteration. Controller is of 11^{th} order and strictly proper in nature. The controller is tested on the closed loop unity feedback TRMS in SIMULINK for computer simulation. Simulation results of the experiments are presented in the next section. All experiments are conducted in the laboratory environment under ideal conditions.

V. Simulation Results - H_∞ Control

As discussed in Section I, TRMS has pitch and yaw movements which are the angular displacements in two perpendicular planes. (No roll is permitted.) If tail position is fixed, pitch output can be observed in a fixed vertical plane. Similarly, if pitch position is fixed in a vertical plane, tail will displace in a plane perpendicular to the pitch plane. In the TRMS setup, if the pitch is given an elevation of 28º from rest, it hovers in the horizontal plane. Although, there is a good range of pitch and yaw angles for which the system shows stability in real time, yet simulation results are presented for pitch angle of 28º and yaw angles of 80º and 210º. The H_∞ controller is simulated for square, sinusoidal and pseudo random noise inputs with few other sets of command inputs before being tested on the actual TRMS. Physical plant is tested for pitch command of 28º and yaw command of 80º.

A. Computer Simulation with Square, Sine and Pseudo Random Noise Inputs

Fig. 7(a) illustrates pitch response to square signal. The outputs of TRMS and second order reference system, $G_{01}(s)$ are compared, here. Fig. 7(b) illustrates control input to main rotor. The control signal to each servo motor is ±18 volts. But, the input to digital to analog interface is bounded within ±2.5 volts. In the latest software versions of TRMS, a built-in saturation block of ±2.5 volts is provided. Fig. 8(a) compares yaw response and output of $G_{02}(s)$ against square command. Yaw displacement is limited to ±210º in horizontal plane in actual plant. Fig. 8(b) illustrates control input to tail rotor.

The bounded control for tail rotor and main rotor are ±2.5 volts, which is shown as a band in Fig. 8(b). The control voltage spikes are taken care by the built-in saturation block. Fig. 9(a) and Fig. 10(a) illustrate responses against sinusoidal inputs. Delay in pitch and yaw outputs may be recorded. Control inputs are well within limit as presented in Fig. 9(b) and Fig. 10(b). Again in Fig. 11(a) and Fig. 12(a), responses against pseudo (band limited) random noise inputs are tested and presented. Notably, the outputs swing around the average values of inputs. Again the control signals are noisy but bounded within specifications. Finally, TRMS is tested in real time against a constant set point. But, before that it is tested by computer simulations as illustrated in Fig. 13 to 15. The control signals are observed to be within limit. Control signal is an indicator of the energy exerted by the system.

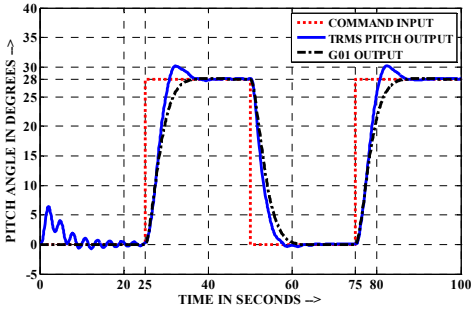

(a)

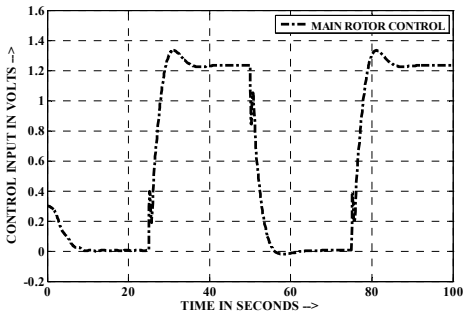

(b)

Fig. 7. (a) Pulse command input of 0.02 Hz – TRMS pitch displacement Vs response of reference plant, $G_{01}(s)$ (b) Main rotor control input in volts for pulse command input.

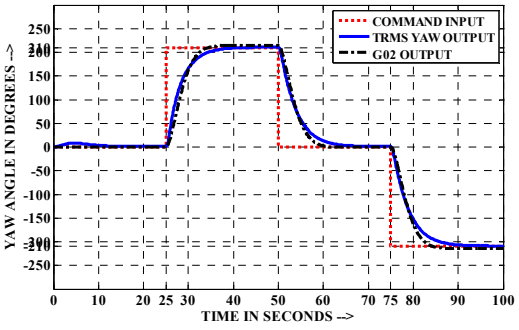

(a)

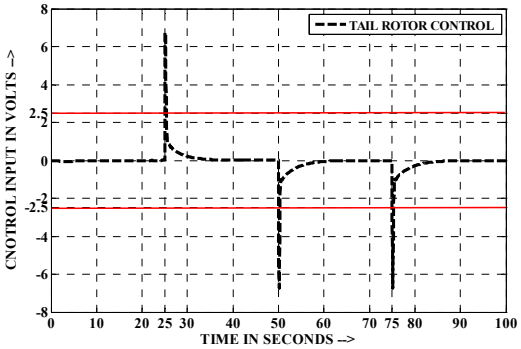

(b)

Fig. 8. (a) Square command input – TRMS yaw displacement Vs response of reference plant, $G_{02}(s)$ (b) Tail rotor control input in volts. Rotor input saturation beyond ±2.5 volts is observed (square command).

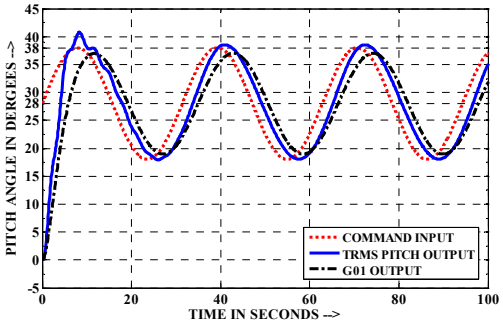

(a)

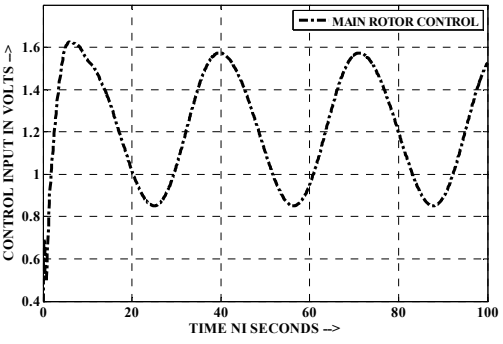

(b)

Fig. 9. (a) Sinusoidal command input of 0.2 radians/second – TRMS pitch displacement Vs response of reference plant, G_{01}. (b) Main rotor control for sinusoidal command input.

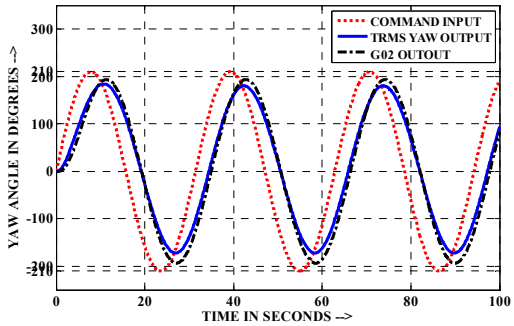

(a)

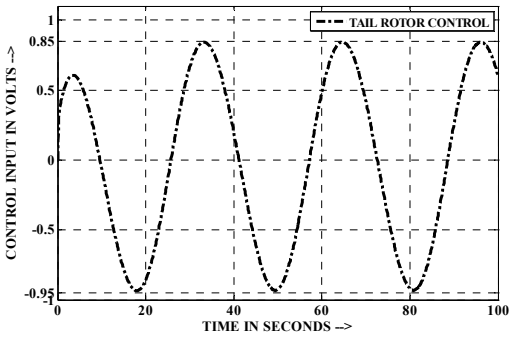

(b)

Fig. 10. (a) Sinusoial command input – TRMS yaw displacement Vs response of reference plant, $G_{02}(s)$. (b) Tail rotor control for sinusoidal command input.

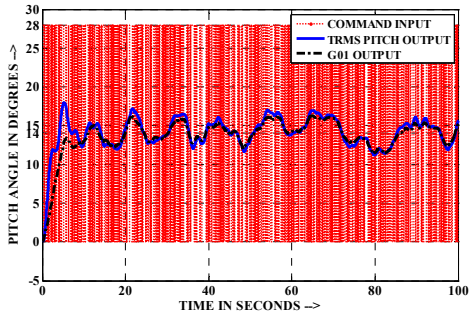

(a)

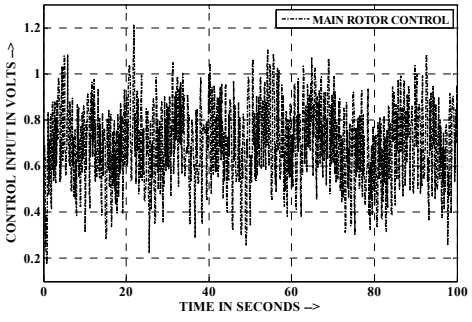

(b)

Fig. 11. (a) Pseudo random noise command input of upper value 28º and frequency 10Hz – TRMS pitch displacement Vs response of reference plant, $G_{01}(s)$. (b) Main rotor control - Pseudo random noise command input of upper value 28º and frequency 10Hz.

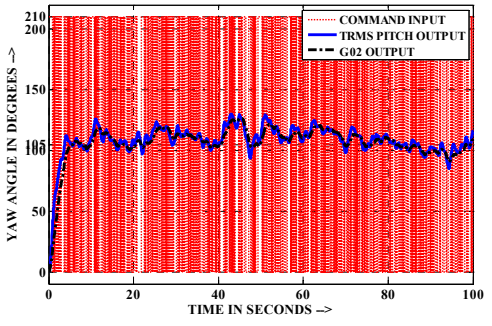

(a)

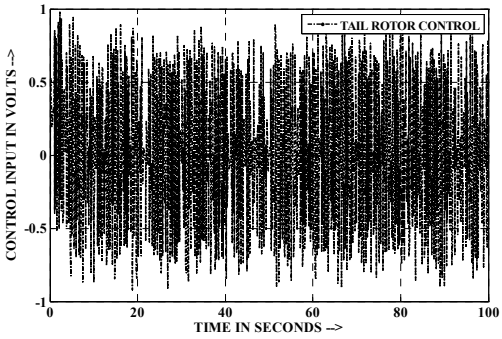

(b)

Fig. 12. (a) Pseudo random noise command input of upper value 210º and frequency 10Hz – TRMS yaw displacement Vs response of reference plant, $G_{02}(s)$. (b) Tail rotor control - Pseudo random noise command input of upper value 210º and frequency 10Hz.

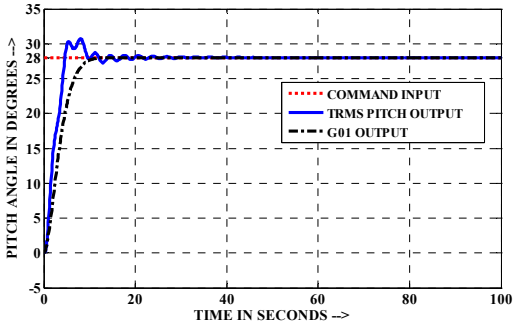

(a)

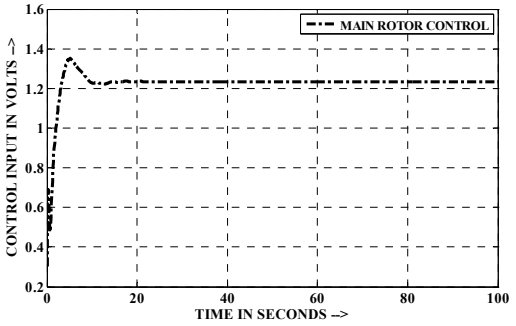

(b)

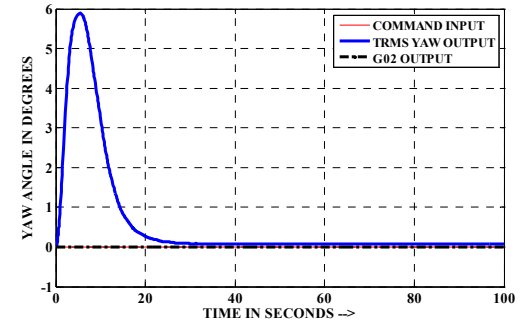

(c)

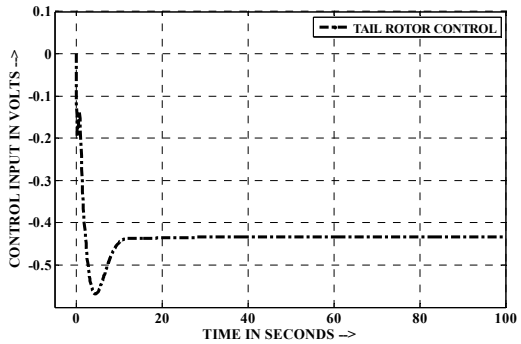

(d)

Fig. 13. (a) TRMS pitch displacement Vs response of reference plant, $G_{01}(s)$ – pitch command 28º and yaw reference 0. (b) Main rotor control – pitch command 28º and yaw reference 0. (c) TRMS yaw displacement Vs response of reference plant, $G_{02}(s)$ – pitch command 28º and yaw reference 0. (d) Tail rotor control – pitch command 28º and yaw reference 0.

In Fig. 13(c), response of G_{02} is not perceptible as G_0 is in canonical form and cross coupling is not present. On the other hand, TRMS has coupling effect, which is cancelled but with delay. Yaw reference is set to command signal of 80º and pitch reference is kept at neutral, as illustrated in Fig. 14(a)-(d). Again, in Fig. 14(a), output of G_{01} is not observed due to the decoupled structure of G_0. Thus, TRMS illustrates coupling between two forward paths. Fig. 14(b) illustrates that command input zero does not imply that control input will also be zero. The control efforts in Fig. 13(d) and Fig. 14(b) are to minimize the cross coupling effects.

In Fig. 14(d), although the upper bound of control input is violated, yet the built-in saturation block protects the physical system from any damage. It is noticed that single spike of control voltage is sufficient to achieve yaw reference angle of 80º. In Fig. 15(a)-(d), pitch reference of 28º and yaw reference of 80º are given simultaneously and outputs are recorded.

B. Control Experiment on Real Time TRMS

The H_∞ controller has demonstrated commendable results as illustrated in Fig. 7 through Fig. 15. Response of TRMS is in close proximity with the second order reference plant as desired.

This 11th order H_∞ controller is further tested on closed loop TRMS in the laboratory environment and outputs are recorded as presented in Fig. 16(a)-(d). The system is tested under nominal conditions, that is, disturbance due to external agencies are neglected. The effect of the output disturbance on pitch and yaw displacements will be presented in an ensuing paper.

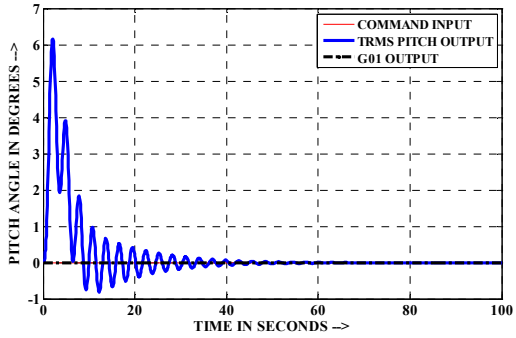

(a)

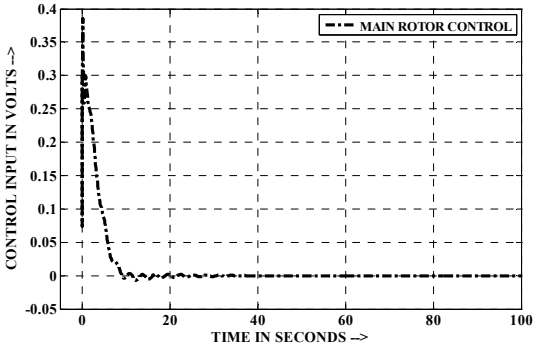

(b)

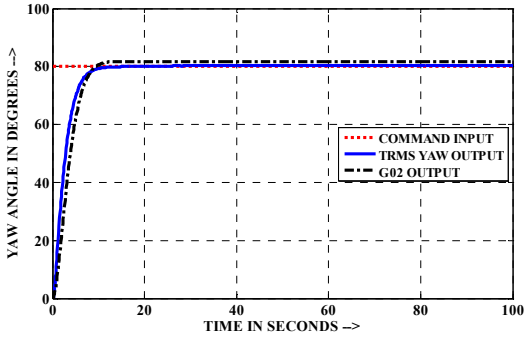

(c)

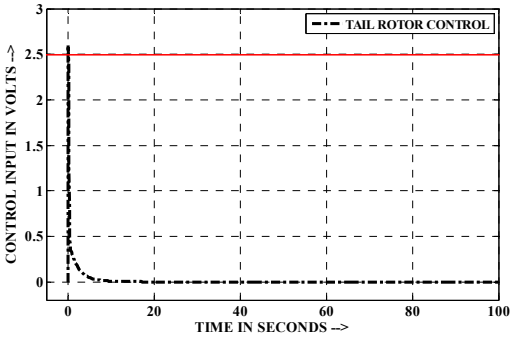

(d)

Fig. 14. (a) TRMS pitch displacement Vs response of reference plant, $G_{01}(s)$ – pitch command 0 and yaw reference 80º. (b) Main rotor control – pitch command 0 and yaw reference 80º. (c) TRMS yaw displacement Vs response of reference plant, $G_{02}(s)$ – pitch command 0 and yaw reference 80º. (d) Tail rotor control – pitch command 0 and yaw reference 80º.

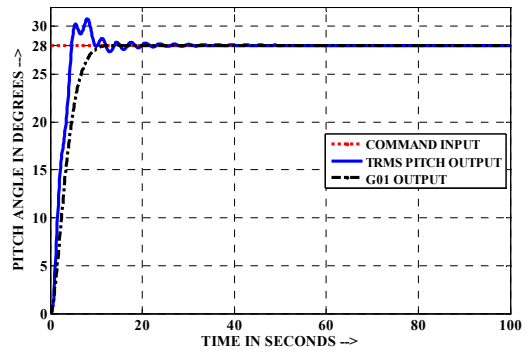

(a)

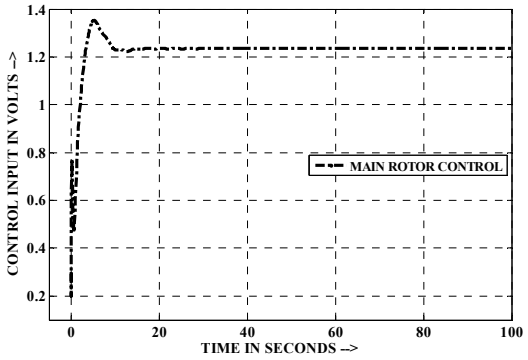

(b)

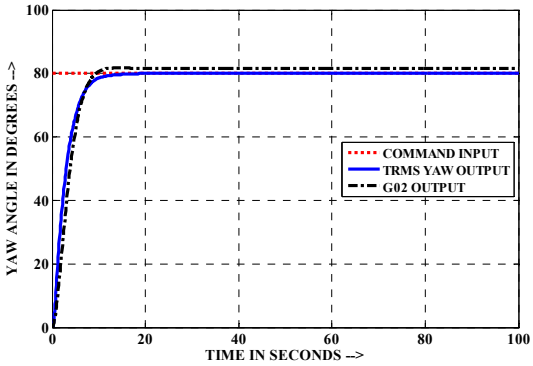

(c)

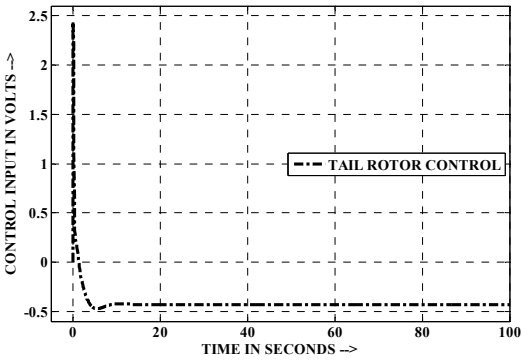

(d)

Fig. 15. (a) TRMS pitch displacement Vs response of reference plant, $G_{01}(s)$ – pitch command 28º and yaw reference 80º. (b) Main rotor control – pitch command 28º and yaw reference 80º. (c) TRMS yaw displacement Vs response of reference plant, $G_{02}(s)$ – pitch command 28º and yaw reference 80º. (d) Tail rotor control – pitch command 28º and yaw reference 80º.

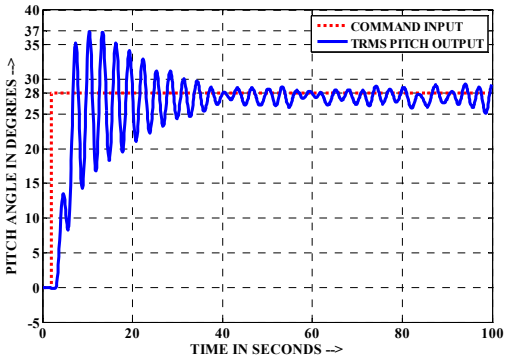

(a)

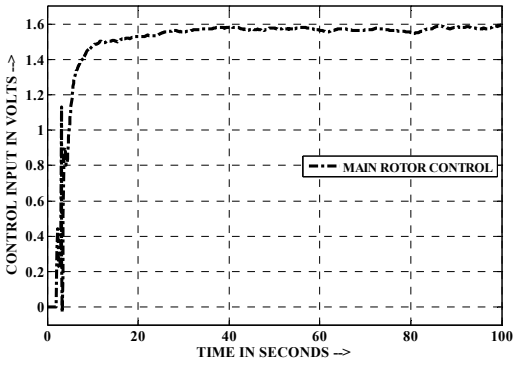

(b)

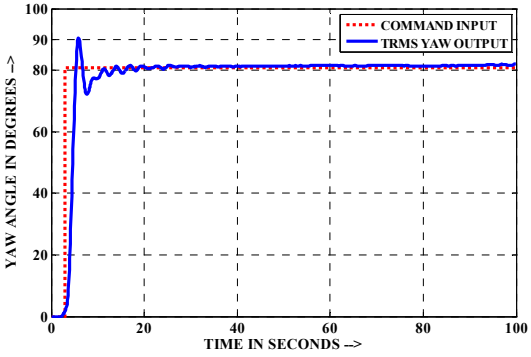

(c)

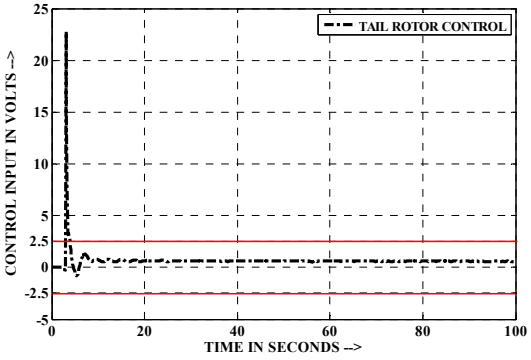

(d)

Fig. 16. (a) TRMS pitch displacement – pitch command 28º and yaw reference 80º in real time. (b) Main rotor control – pitch command 28º and yaw reference 80º. (c) TRMS yaw displacement – pitch command 28º and yaw reference 80º in real time. (d) Tail rotor control – pitch command 28º and yaw reference 80º.

C. Analysis of Test Results

The experiments on TRMS in Fig. 15 and 16 have illustrated acceptable results on relative and absolute stability parameters. Tables 5 and 6 compare pitch and yaw outputs, respectively. The controlled amplitude at the natural frequency (0.346 Hz) is observed as ripple at pitch output of real time experiment in steady state, as in [1]-[4]. The delay and inverse responses are observed in both the cases, that is, computer simulation and real time experiment. Control signals are well within bound illustrating energy efficient control, again both in computer simulation and real time cases.

TABLE V. COMPARISON OF RELATIVE STABILITY PARAMETERS - PITCH

Sl. No.	**Relative Stability Parameters of TRMS**		
	Name of parameter	***Simulation***	***Real time***
1.	Rise time (10% to 90%)	3.4 seconds	3.2 seconds
2.	%Peak overshoot	9.929	25
3.	Settling time (2%)*	9.3 seconds	36.2 seconds
4.	Delay**	0.035 seconds	0.4 seconds
5.	%Steady state error*	0.071	1.786
6.	Time to reach second high frequency zero	6.6 seconds	2.5 seconds
*Output ripple in real time pitch response is neglected. **Recorded from experimental data.			

TABLE VI. COMPARISON OF RELATIVE STABILITY PARAMETERS - YAW

Sl. No.	**Relative Stability Parameters of TRMS**		
	Name of parameter	***Simulation***	***Real time***
1.	Rise time (10% to 90%)	5.52 seconds	1.4 seconds
2.	%Peak overshoot	Zero	13
3.	Settling time (2%)*	10.2 seconds	12.3 seconds
4.	Delay**	Zero	Zero
5.	%Steady state error*	0.094	2.088
*Output ripple in real time yaw response is neglected. **Recorded from experimental data.			

It is inferred from Tables 5 and 6 that all parameter values are scaled up in case of actual plant. The possible causes are modeling and scaling errors.

VI. CONCLUSION

This paper has presented a matrix modulation technique on a conceptual plant, known as generalized plant or four block plant in control literature, for convergence of H_∞ control algorithm. The convergence is ensured by populating the sub-matrices of the generalized plant by artificial augmentation of certain signals (vectors) at design stage. This approach reduces the requirement of augmenting certain hardware loops in the actual plant in order to mitigate the signal singularities. Thus, the matrix inversion issues are transformed to signal singularities. The optimization is based on output error regulation of a model matching problem. The H_∞ controller, developed in this way, is tested on the TRMS by computer simulation followed by real time experiment. The illustrations of modeling and scaling errors, RHP zeros, delays, and natural modes in the outputs imply further research opportunities in this area. In light of the high order of the controllers and its hardware implementation issues, the controller model reduction approach will be duly addressed in an ensuing paper. It may further be added that helicopter technology has developed in many centuries and thus migration from mechanical era to the electrical world may engage at least another few decades.

ACKNOWLEDGMENT

This work was performed in the Control Systems laboratory of the Electrical Engineering Department at National Institute of Technology Calicut, India. The authors are thankful to the technical staff of the Institute for providing the experimental support, facilities and arrangement. The authors appreciate the valuable comments from the reviewers.

REFERENCES

[1] S. M. Ahmad, A. J. Chipperfield, and M. O. Tohki, "Modelling and control of a twin rotor multi-input multi- output system," in Proc. American Control Conference, pp. 1720-1724, 2000.

[2] S. M. Ahmad, A. J. Chipperfield, and M. O. Tohki, "Dynamic modelling and optimal control of a twin rotor mimo system," in Proc. IEEE, pp. 391-398, 2000.

[3] S. M. Ahmad, A. J. Chipperfield, and M. O. Tohki, "Dynamic modelling and linear quadratic Gaussian control of a twin-rotor multi-input multi-output system," in Proc. Instn. Mech. Engrs, Journal of Systems and Control Engineering, vol. 217, part I, pp. 203-227, 2003.

[4] P. K. Paul, and J. Jacob, "On the modeling of twin rotor MIMO system using chirp inputs as test signals," Asian Journal of Control, vol. 19, no. 6, pp. 1–10, November 2017.

[5] G. Zames, "Feedback and optimal sensitivity: model reference transformation, multiplicative seminorms, and approximate inverses," IEEE Trans. Autom. Control, vol. AC-26, no. 2, pp. 301-320, April 1981.

[6] K. Zhou, and P. P. Khargonekar, "An algebraic Riccati equation approach to H_∞ optimization," Syst. & Control Letters, North Holland, vol. 11, pp. 85-91, 1988.

[7] M. Sampei, T. Mita, and M. Nakamichi, "An algebraic approach to H_∞ output feedback control problems," Syst. & Control Letters, North Holland, vol. 14, 13 – 24, 1990.

[8] T. Iwasaki , and R. E. Skelton, "All controllers for the general H_∞ control problem: LMI existence conditions and state space formulas," Automatica, Great Britain, vol. 30, no. 8, pp. 1307 – 1307, 1994.

[9] J. C. Doyle, K. Glover, P. P. Khargonekar, and B. A. Francis, "State-space solutions to standard H_2 and H_∞ control problems," IEEE Trans. Autom. Control, vol. 34, no. 8, pp. 831 – 847, 1989.

[10] A. Megretski, "On the order of optimal controllers in the mixed H-2/H-infinity control," in Proc. 33rd Conf. Decis. Control, Lake Buena Vista, Florida, pp. 3173-3174, 1994.

[11] M. L. Martinez, C. Viva, and M. G. Ortega, "A multivariable nonlinear H_∞ controller for a laboratory helicopter," in Proc. 44th IEEE Conf. on Decision and Control, pp. 4065-4070, 2005.

[12] M. L. Martinez, C. Vivas, M. G. Ortega, and F. R. Rubio, "Nonlinear L2 control of a laboratory helicopter with variable speed rotors," Automatica, vol. 43, pp. 655 – 661, 2007.

[13] Ph. Mullhaupt, B. Srinivasan, J. Levine, and D. Bonvin, "Cascade control of the toycopter," in Proc. European Control Conf. (ECC'99), Karlsruhe, pp. 3226 – 3231, 1999.

[14] S. F. Toha, and M. O. Tokhi, "Inverse model based control for a twin rotor system," IEEE 9th Int. Conf. Cybernetic Intelligent Systems, UK, pp. 1-5, September 2010.

[15] J. P. Su, C. Y. Liang, and H. M. Chen, "Robust control of a class of nonlinear systems and its application to a twin rotor MIMO system,"

IEEE Int. Conf. on ICIT, Bangkok, Thailand, vol. 2, pp. 1272-1277, 2002.

[16] P. K. Paul, and J. Jacob, "Elevation and hovering control of TRMS via H_∞ optimization technique," 1st IEEE Int. Conf. ICPEICES, New Delhi, India, pp. 1-6, 2016.

[17] A. Rahideh, M. H. Shaheed, and H. J. C. Huijberts, "Dynamic modelling of a TRMS using analytical and empirical approaches," Control Eng. Practice, vol. 16, pp. 241–259, 2008.

[18] T. W. Lu, and P. Wen, "Time optimal and robust control of twin rotor system," IEEE Int. Conf. Control Automation, vol. ThA3-2, pp. 862-866, 2007.

[19] Feedback Instruments Ltd., Twin rotor MIMO system control experiments 33-949S Laboratory Manual, U.K., 2005.

[20] S. Skogestad, and I. Postlethwaite, Multivariable Feedback Control - Analysis and Design, 2nd ed., John Wiley and Sons, England, , 2005.

[21] D. U. C. Delgado, and K. Zhou, "A parametric optimization approach to H_∞ and H_2 strong stabilization," Automatica, vol. 39, pp. 1205-1211, 2003.